Journal of Photonics for Energy

PhotonicsforEnergy.SPIEDigitalLibrary.org

Solvent-dependent investigation of carbazole benzonitrile derivatives: does the ^{3}LE – ^{1}CT energy gap facilitate thermally activated delayed fluorescence?

Takuya Hosokai
Hiroki Noda
Hajime Nakanotani
Takanori Nawata
Yasuo Nakayama
Hiroyuki Matsuzaki
Chihaya Adachi

SPIE.

Takuya Hosokai, Hiroki Noda, Hajime Nakanotani, Takanori Nawata, Yasuo Nakayama, Hiroyuki Matsuzaki, Chihaya Adachi, "Solvent-dependent investigation of carbazole benzonitrile derivatives: does the ^{3}LE – ^{1}CT energy gap facilitate thermally activated delayed fluorescence?," *J. Photon. Energy* **8**(3), 032102 (2018), doi: 10.1117/1.JPE.8.032102.

Solvent-dependent investigation of carbazole benzonitrile derivatives: does the ^{3}LE – ^{1}CT energy gap facilitate thermally activated delayed fluorescence?

Takuya Hosokai,[a,*] Hiroki Noda,[b] Hajime Nakanotani,[b,c,d] Takanori Nawata,[e] Yasuo Nakayama,[e] Hiroyuki Matsuzaki,[a] and Chihaya Adachi[b,c,d]

[a]National Metrology Institute of Japan (NMIJ), National Institute of Advanced Industrial Science and Technology (AIST), Tsukuba, Ibaraki, Japan

[b]Kyushu University, Center for Organic Photonics and Electronics Research (OPERA), Nishi, Fukuoka, Japan

[c]Kyushu University, Japan and International Institute for Carbon Neutral Energy Research (WPI-I2CNER), Nishi, Fukuoka, Japan

[d]Kyushu University, JST, ERATO, Adachi Molecular Exciton Engineering Project, c/o OPERA, Nishi, Fukuoka, Japan

[e]Tokyo University of Science, Department of Pure and Applied Chemistry, Faculty of Science and Technology, Noda, Japan

Abstract. The photophysical properties of six types of carbazole benzonitrile (CzBN) derivatives are investigated in different solvents to examine the thermally activated delayed fluorescence (TADF) activation via reducing the energy gap between the singlet charge-transfer and triplet locally excited states, $\Delta E_{ST(LE)}$. Relative to the $\Delta E_{ST(LE)}$ values for the CzBN derivatives in the low polarity solvent toluene ($\varepsilon \sim 2$), a reduction of $\Delta E_{ST(LE)}$ for the CzBN derivatives in the polar solvent acetonitrile ($\varepsilon \sim 37$) was confirmed while maintaining fairly constant ΔE_{ST} values. Notably, TADF activation was observed in acetonitrile for some CzBN derivatives that are TADF inactive in toluene. A numerical analysis of various rate constants revealed the cause of TADF activation as an increase in the reverse intersystem crossing rate and a suppression of the non-radiative decay rate of the triplet states. The positive effect of $\Delta E_{ST(LE)}$ was limited, however, as an excessive decrease in $\Delta E_{ST(LE)}$ facilitates the nonradiative deactivation of the triplet states, leading to a loss of the TADF efficiency. This paper shows that $\Delta E_{ST(LE)}$ provides a measure of TADF activation and that appropriate regulation of $\Delta E_{ST(LE)}$ is required to achieve high TADF efficiency. [DOI: 10.1117/1.JPE.8.032102]

Keywords: thermally activated delayed fluorescence; CzBN derivatives; photophysical properties; singlet–triplet energy gap.

Paper 17120SS received Nov. 14, 2017; accepted for publication Jan. 8, 2018; published online Feb. 2, 2018.

1 Introduction

Thermally activated delayed fluorescence (TADF) of organic molecules has attracted tremendous attention owing to its potential application to organic light-emitting diodes (OLEDs) and has also renewed interest in photochemistry and photophysics.[1,2] Uoyama et al.[3] established a design concept for the synthesis of highly efficient TADF molecules by connecting electron-donating and -accepting substituents with a large torsion angle. Such a structure can separate the wavefunction overlap between the highest occupied molecular orbital and the lowest unoccupied molecular orbital, leading to a significant reduction in the energy gap (ΔE_{ST}) between the first

*Address all correspondence to: Takuya Hosokai, E-mail: t.hosokai@aist.go.jp

excited singlet state (S_1) and the first excited triplet state (T_1). Notably, the ΔE_{ST} diminishes to thermal energy at room temperature, ~25 meV, and typically <100 meV. Thus, this approach affords a thermal pathway to convert from the T_1 state to the S_1 state via reverse intersystem crossing (RISC), thereby facilitating TADF. After Uoyama's report,[3] a number of TADF molecules were rapidly synthesized and exhibited a high internal photoluminescence quantum yield (PLQY) of TADF (Φ_{DF}) in various emission colors, including blue.[4–10] Additionally, the device performance of OLEDs, such as external electroluminescence quantum efficiency and operational stability, is being improved by this approach.[11–14]

In addition to these exciting applications of TADF, the fundamental processes in TADF are also attracting considerable interest in both experimental and theoretical fields.[15–26] In this case, the goal is to achieve a sufficient understanding of these processes to realize a high RISC rate (k_{RISC}) by judicious designing and optimizing the most suitable chemical structures, emission environments, and so on. Increasing the k_{RISC} suppresses triplet state quenching and is, therefore, beneficial for reducing roll-off in OLEDs and organic laser diodes.[27–29]

One important question of the TADF mechanism concerns the rate of the various electron transfer processes. That is, although ΔE_{ST} values at thermal energy or even less have been attained, and intersystem crossing rates (k_{ISC}) as high as 10^8 s^{-1} have been obtained, the corresponding k_{RISC} values were often limited to a maximum of 10^6 s^{-1}. Moreover, Φ_{DF} values close to 80% were achieved, even with a relatively appreciable ΔE_{ST} value of ~0.2 eV.[24] Theoretical simulations have indicated that selecting certain molecular orbitals between the S_1 and T_1 states is essential to achieve a high k_{RISC}; known as El-Sayed's rule, it has been shown that high k_{RISC} values can be achieved by exploiting the singlet charge-transfer (^{1}CT) and triplet locally excited (^{3}LE) states.[18,19,21,25] In addition, some groups have proposed that second-order spin-orbit coupling enables utilization of higher order triplet states, which further facilitates RISC.[18,20,23] Conventional and time-dependent density functional theory calculations based on such orbital selection rules and/or second-order perturbation theory have succeeded in reproducing the experimentally determined k_{RISC} values of some, but not all, of the organic molecules investigated.[21] Thus, a broad consensus of the TADF mechanism has yet to be reached.

Another aspect of the selection rules for RISC is our recent proposal based on experimental data that the energy gap between ^{1}CT and ^{3}LE, so-called $\Delta E_{ST(LE)}$, is an important parameter to signify TADF [Fig. 1(a)].[24] The carbazole benzonitrile (CzBN) derivatives 2CzBN, *o*-3CzBN, *m*-3CzBN, *p*-3CzBN, 4CzBN, and 5CzBN [Fig. 1(b)] have shown relatively similar ΔE_{ST} values of ~0.2 eV, as determined by their corresponding fluorescence and phosphorescence spectra, together with fairly different k_{RISC} values from zero to 10^5 s^{-1}.[24] Assuming that their ^{3}LE values are similar, which arise from structurally common Cz moieties (vide infra), the $\Delta E_{ST(LE)}$ values estimated from the ^{3}LE(Cz) and ^{1}CT levels of each CzBN derivative varied from −0.06 to 0.23 eV because of different ^{1}CT levels for each CzBN derivative. As a result, $\Delta E_{ST(LE)}$ and k_{RISC}, but not ΔE_{ST}, were found to be correlated; specifically, decreasing values of $\Delta E_{ST(LE)}$ lead to an increase in k_{RISC}. For this reason, $\Delta E_{ST(LE)}$ was proposed as an additional measure, in conjunction with ΔE_{ST}, for determining whether molecules could exhibit TADF. However, further investigations are needed to verify the generality of this concept; in particular, it is desirable to establish whether tuning $\Delta E_{ST(LE)}$ can indeed facilitate TADF and vice versa.

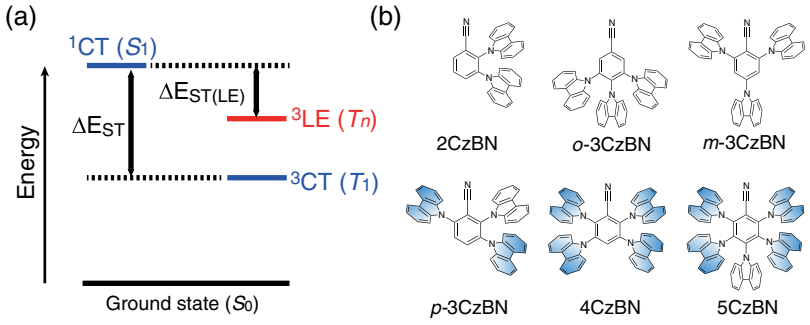

Fig. 1 (a) Definition of ΔE_{ST} and $\Delta E_{ST(LE)}$. (b) Chemical structures of CzBN derivatives.

In this paper, we investigated the solvent dependence of the photophysical properties of six types of CzBN derivatives. It is known that a host matrix can tune CT state energies and that large environmental dielectric fields stabilize CT states by orienting the polarization of the surrounding solvent. Notably, LE states are hardly affected by this phenomenon.[30] This means that selecting the type of host matrix (e.g., solvent) can modulate the energy levels of CzBN derivatives and give rise to different photophysical properties. We previously investigated the photophysical properties of CzBN derivatives in toluene, whose dielectric constant (ε) is ~2 at room temperature. In the present study, the strong polar solvent acetonitrile ($\varepsilon \sim 37$) was used to investigate the photophysical properties of the same six CzBN derivatives, the results of which are compared with the previous results determined in toluene.[24] The large ε of acetonitrile is expected to stabilize the ^{1}CT and ^{3}CT states and, thus, tune the energy levels, in particular $\Delta E_{ST(LE)}$, of the CzBN derivatives.

2 Experimental

All the materials were synthesized according to Ref. 24 and purified by thermal sublimation. Solutions were prepared by dissolving the purified molecules in toluene or acetonitrile, both of which were of spectrochemical analysis grade (purity: 99.8%, Wako Pure Chemical Industries, Ltd.). The solution concentration ranged from 10^{-4} to 10^{-5} M depending on the samples.

Optical properties of the solutions were characterized by measuring the steady-state ultraviolet-visible (UV-vis) absorption/PL spectra and transient PL decay curves (hereafter called transient PL). UV-vis absorption spectra were acquired using a UV-VIS-NIR scanning spectrophotometer (UV-3100PC, Shimazu), whereas PL spectra were recorded using a fluorescence spectrophotometer (LS50B, Perkin Instruments or Lambda 950-PKA Instrument, Perkin–Elmer). Transient PLs were measured using a fluorescence lifetime spectrometer (C11367-01, Hamamatsu Photonics or a FluoroCube, Horiba). The PLQY of the solutions was measured using an absolute PLQY measurement system (C11347-01, Hamamatsu Photonics) with an excitation wavelength of 337 nm under two conditions: as prepared and after degassing by dry argon gas to eliminate triplet state deactivation. Before the transient PL measurements, the solutions were also deoxygenated with dry nitrogen or argon gas for the same reason. The triplet state lifetime of 2CzBN in acetonitrile was determined by microsecond-transient absorption spectroscopy using the third harmonic of fundamental light (1064 nm) of a Nd^{3+} : YAG laser as the pump light (wavelength, 355 nm; FWHM pulse, <150 ps; repetition, 10 Hz) and a xenon steady-state lamp as the probe light. Full details of this design are described in Ref. 31. The irradiated intensity of the pump laser was set to 0.7 mJ/cm^2.

3 Results and Discussion

Figures 2(a)–2(f) show the UV–vis absorption, fluorescence, and phosphorescence spectra of the six CzBN derivatives in toluene (upper) and acetonitrile (bottom). In the absorption spectra, $\pi - \pi^*$ transitions at a single Cz moiety [$Cz(\pi - \pi^*)$] are commonly observed in the UV region (3.7 to 4.0 eV). Below this region, two types of CT transitions are observed depending on the molecules: CT1, which originates from a CT transition from one Cz moiety to the center BN moiety, located at ~3.4 to 3.6 eV, and CT2, which is a CT transition among two Cz moieties at para-positions [2 and 5 or 3 and 6, see blue-colored Czs in Fig. 1(b)] and the BN moiety at the lowest energy region (~3.0 to 3.2 eV).[24] Both CT transitions are apparent in the absorption spectrum of 5CzBN [Fig. 2(f)]. Their formation in 5CzBN can be understood in terms of its chemical structure, which is composed of two para-Cz pairs and a single Cz moiety opposite the cyano group; collectively, these structural features fulfill the electronic condition of both CT transitions. By comparison, only the CT1 transition was present in the spectra of 2CzBN, *o*-3CzBN, and *m*-3CzBN, and only the CT2 transition was evident in the spectra of *p*-3CzBN and 4CzBN. In terms of their molecular structures, the former three have no such Cz pairs, and the latter two possess Cz pairs. The structure-dependent absorption of the CzBN derivatives in toluene was also observed viz. their corresponding transient absorption spectra, as reported in Ref. 24.

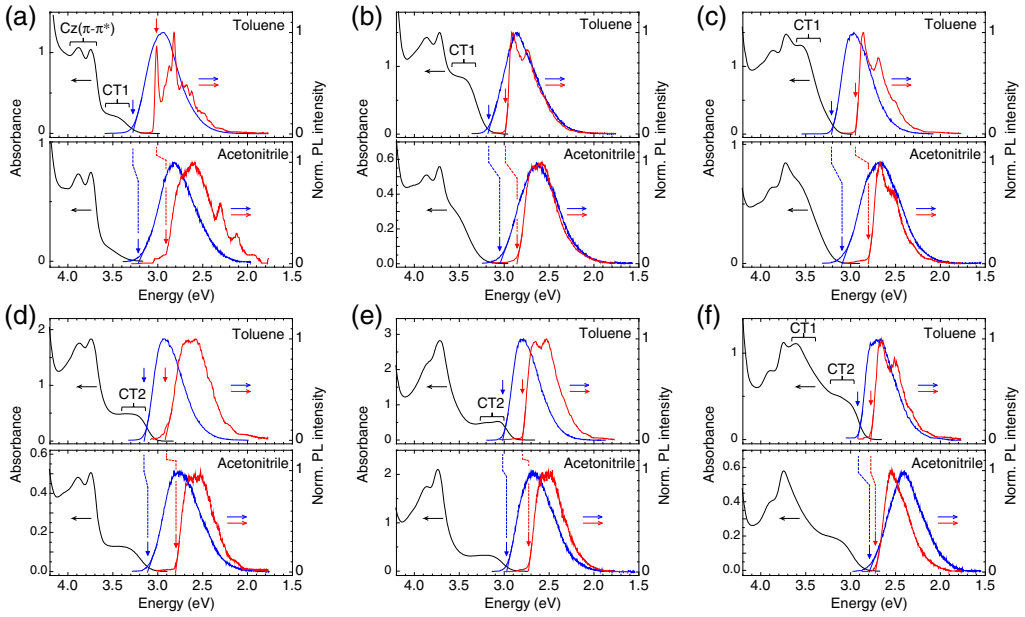

Fig. 2 UV–vis absorption, fluorescence, and phosphorescence (77 K) spectra of (a) 2CzBN, (b) *o*-3CzBN, (c) *m*-3CzBN, (d) *p*-3CzBN, (e) 4CzBN, and (f) 5CzBN in toluene (upper) and acetonitrile (bottom). Threshold (or partial peak top) energies in the fluorescence and phosphorescence spectra are depicted by blue or red vertical arrows, respectively.

The three distinct absorption features in Figs. 2(a)–2(f) [i.e., Cz ($\pi - \pi^*$), CT1, and CT2] indicate different photophysical behavior of the CzBN derivatives in toluene and acetonitrile. The peak positions of the Cz ($\pi - \pi^*$) transition remain almost unchanged, whereas both the CT1 and CT2 transitions exhibit a blue shift and a decrease in intensity in acetonitrile. Moreover, the intensity decrease is much stronger for CT1 compared with CT2; for instance, the peak structure of the CT1 transition changes to a shoulder-like feature in acetonitrile for 5CzBN. These results suggest that both the CT1 and CT2 transitions contain $n - \pi^*$ character, but the solvent effect differs between local CT (CT1) and delocalized (at para-Cz pairs) CT (CT2), presumably due to the distinct electron distributions in their excited states.

Solvent effects were also evident in the fluorescence and phosphorescence spectra of the six CzBN derivatives. Essentially, both the fluorescence and phosphorescence spectra show a red shift in acetonitrile, as seen in Figs. 2(a)–2(f), which we attribute to stabilization of both the ^{1}CT and ^{3}CT states. Only the phosphorescence spectrum of 2CzBN in toluene exhibits distinctly sharp vibronic progressions, which are attributable to emission from ^{3}LE in the Cz moieties.[24] This result also suggests that the ^{3}LE state of 2CzBN in toluene is lower in energy than the ^{3}CT state. By comparison, the phosphorescence spectrum of 2CzBN in acetonitrile is rather broadened, suggesting an exchange of the T_1 from ^{3}LE to ^{3}CT or an increase of electronic coupling between the two states, i.e., the strengthening of state mixing, due to their energy proximity because of the ^{3}CT stabilization.[32,33]

On the basis of the fluorescence and phosphorescence results, the ΔE_{ST} and $\Delta E_{ST(LE)}$ values of each CzBN derivative were estimated and are given in Table 1, where the S_1 and T_1 energies used for the estimation are also depicted. For the $\Delta E_{ST(LE)}$, the energy of the ^{3}LE state in the phosphorescence spectrum of 2CzBN was used, as with our previous report.[24] Here we note that both the ΔE_{ST} and $\Delta E_{ST(LE)}$ values in the toluene samples are slightly differed from the previous reports owing to the use of different apparatus and measurement conditions. As seen in Table 1, the ΔE_{ST} values in toluene range from 0.16 to 0.27 eV, and these values are not appreciably reduced in acetonitrile, except for 5CzBN; in this case, 5CzBN showed a decrease in ΔE_{ST} from 0.16 to 0.07 eV. In this context, the k_{RISC} value of only 5CzBN is anticipated to increase according to the relation between ΔE_{ST} and k_{RISC}: $k_{RISC} \sim 1/\exp(\Delta E_{ST}/kT)$, where k is the Boltzmann constant and T is the temperature. However, as will be shown, this expectation is misleading because k_{RISC} is actually influenced significantly by $\Delta E_{ST(LE)}$. As expected

Table 1 ΔE_{ST} and $\Delta E_{ST(LE)}$ of CzBN derivatives in toluene and acetonitrile.

		2CzBN	*o*-3CzBN	*m*-3CzBN	*p*-3CzBN	4CzBN	5CzBN
ΔE_{ST} (eV)[a,c]	Toluene	0.26	0.18	0.27	0.24	0.22	0.16
	Acetonitrile	0.31	0.19	0.29	0.31	0.25	0.07
$\Delta E_{ST(LE)}$ (eV)[b,c]	Toluene	0.26	0.16	0.20	0.14	0.01	−0.08
	Acetonitrile	0.21	0.04	0.09	0.10	−0.04	−0.22
S_1 level (eV)	Toluene	3.27	3.17	3.21	3.15	3.02	2.93
	Acetonitrile	3.22	3.05	3.10	3.11	2.97	2.79
T_1 level (eV)	Toluene	3.01	2.99	2.95	2.92	2.80	2.78
	Acetonitrile	2.91	2.86	2.80	2.80	2.72	2.72

[a]Energy gap calculated from the S_1 and T_1 energy levels estimated from the threshold of the fluorescence spectra and peak (2CzBN in toluene) or threshold (2CzBN in acetonitrile and other CzBN derivatives) of the phosphorescence spectra, respectively [Figs. 2(a)–2(f)].
[b]Energy gap calculated from the ^{1}CT (S_1) and ^{3}LE (T_1 of 2CzBN in toluene), respectively.
[c]The error bar of ΔE_{ST} and $\Delta E_{ST(LE)}$ is a maximum of ±0.05 eV.

from the decrease in the ^{3}CT energies, the $\Delta E_{ST(LE)}$ values of all the CzBN derivatives decreased in acetonitrile. In particular, the $\Delta E_{ST(LE)}$ values of *o*-3CzBN and *m*-3CzBN are reduced largely from 0.16 to 0.04 eV and from 0.20 to 0.09 eV, respectively. These values are less than that of *p*-3CzBN examined previously, which was the only isomer of the three that showed TADF in toluene.[24] On the basis of the present results, TADF is expected to be active for *o*-3CzBN and *m*-3CzBN in acetonitrile.

To examine the $\Delta E_{ST(LE)}$ values in the context of TADF properties, we next discuss the results of transient PL for all the sample solutions. As seen in Figs. 3(a)–3(f), the transient PL measured for toluene (red line) are indicated in the bottom axes as a function of their delay time, whereas those of acetonitrile (blue line) are indicated in the upper axes. Note that the time scale for the three 3CzBN isomers differs by orders of magnitude in toluene (μs) and acetonitrile (ms). As expected from the results of $\Delta E_{ST(LE)}$, *o*-3CzBN and *m*-3CzBN, which are TADF inactive in toluene, become TADF active in acetonitrile. Delayed PL components with time constants (τ_{DF}) of 66 and 220 μs for *o*-3CzBN [Fig. 3(b)]

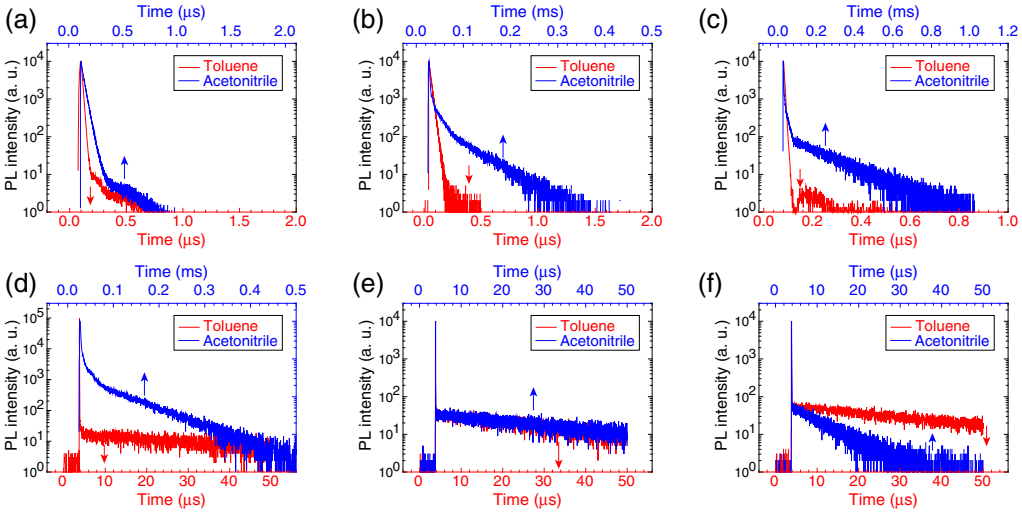

Fig. 3 Comparison of transient PL of CzBN derivatives in toluene (red line, bottom axis) and acetonitrile (blue line, upper axis): (a) 2CzBN, (b) *o*-3CzBN, (c) *m*-3CzBN, (d) *p*-3CzBN, (e) 4CzBN, and (f) 5CzBN.

and *m*-3CzBN [Fig. 3(c)], respectively, were confirmed. These τ_{DF} values are comparable with that of *p*-3CzBN in acetonitrile [103 μs, Fig. 3(d)]. Importantly, Φ_{DF} of the three 3CzBN isomers are similar: 21% for *o*-3CzBN, 18% for *m*-3CzBN, and 24% for *p*-3CzBN. These values were calculated by subtracting the PLQY in air ($\Phi_{PL,air}$) from the PLQY measured after argon bubbling ($\Phi_{PL,degassed}$). After analyzing the photophysical properties of all the solution samples according to Ref. 27, the values of k_{RISC} are obtained as 3.0×10^4 s^{-1} for *o*-3CzBN, 6.4×10^3 s^{-1} for *m*-3CzBN, and 2.1×10^4 s^{-1} for *p*-3CzBN. The k_{RISC} of *p*-3CzBN is slightly improved from 1.3×10^4 s^{-1} in toluene, but that of *o*-3CzBN and *m*-3CzBN improved at least 1 to 2 orders of magnitude, based on the assumption that 10^2 s^{-1} is a lower limit of our estimation. These results clearly indicate that a smaller $\Delta E_{ST(LE)}$ increases the value of k_{RISC}, thereby facilitating TADF. Therefore, TADF can be triggered from being inactive to active by environmental effects. Note that the $\Delta E_{ST(LE)}$ value of 0.20 eV for 2CzBN in acetonitrile is still too large for TADF to develop.

It seems that the effect of reducing $\Delta E_{ST(LE)}$ on k_{RISC} is limited, as the k_{RISC} values of 4CzBN and 5CzBN improved only slightly from 1.8×10^5 s^{-1} to 2.1×10^5 s^{-1} and from 2.4×10^5 s^{-1} to 2.6×10^5 s^{-1} in acetonitrile, respectively. This observation may be deduced from the fact that their $\Delta E_{ST(LE)}$ values become more negative, which means that the ^{3}LE state lies farther from the ^{1}CT state in acetonitrile. This negative shift in $\Delta E_{ST(LE)}$ does not impact the Φ_{DF} value of 4CzBN, although it does significantly decrease the Φ_{DF} value of 5CzBN from 76% in toluene to 24% in acetonitrile. This decrease is caused by an increase in the nonradiative decay rate from T_1 to the ground state (S_0) ($k_{nr,T}$) from 4.2×10^3 s^{-1} (in toluene) to 9.3×10^4 s^{-1} (in acetonitrile). As mentioned above, however, k_{RISC} does not decrease in acetonitrile, indicating that coupling between the ^{3}LE and ^{1}CT states is important for RISC.

Additionally, it is instructive to discuss the impact of the solvent effect for other rate constants relevant to the electron transfer processes in the six CzBN molecules examined. In acetonitrile, the radiation decay rate from S_1 to S_0 ($k_{r,S}$) and k_{ISC} tends to decrease (Table 2). However, this is not the cause of the increase in the nonradiative decay rate for the S_1 to S_0 transition ($k_{nr,S}$), since the $\Phi_{PL,air}$ of the CzBN derivatives, which assumes a PLQY of prompt fluorescence, remains unchanged or even increases, except for 2CzBN and *o*-3CzBN. Although $k_{nr,T}$ of 5CzBN is

Table 2 Photophysical properties of the CzBN derivatives.

		$\Phi_{PL,air}$/ $\Phi_{PL,degassed}$ (%)	Φ_{DF} (%)	τ_{pr}/τ_{DF} (ns)/(μs)	$k_{r,S}$ (10^6 s^{-1})	$k_{nr,T}$ (10^3 s^{-1})	k_{ISC} (10^7 s^{-1})	k_{RISC} (10^3 s^{-1})
2CzBN	Toluene	15/23	0	10.9/1.3[a]	13.8	783[a]	7.8	0
	Acetonitrile	9/20	0	12.4/47.5[a]	7.3	21.1[a]	7.3	0
o-3CzBN	Toluene	21/31	0	18.5/15[a]	11.4	65[a]	4.3	0
	Acetonitrile	12/33	21	14.3/66.2	8.4	11.5	6.2	30.0
m-3CzBN	Toluene	15/17	0	3.6/39[a]	41.7	26[a]	23.6	0
	Acetonitrile	15/33	18	10.1/220.3	14.9	3.6	8.4	6.4
p-3CzBN	Toluene	10/14	4	1.2/35	83.3	27	75.0	12.7
	Acetonitrile	13/37	24	9.6/102.7	13.6	7.0	9.1	20.6
4CzBN	Toluene	9/62	53	1.6/36	56.3	17	56.9	179.8
	Acetonitrile	9/73	64	5.4/36.9	16.6	8.0	16.8	212.0
5CzBN	Toluene	9/85	76	3.8/39	23.7	4.2	23.9	237.9
	Acetonitrile	14/38	24	16.2/7.8	8.6	93.0	5.3	257.0

[a]Virtual values as determined by measuring the triplet-state absorption decay curve in microsecond-TAS (see Ref. 24).

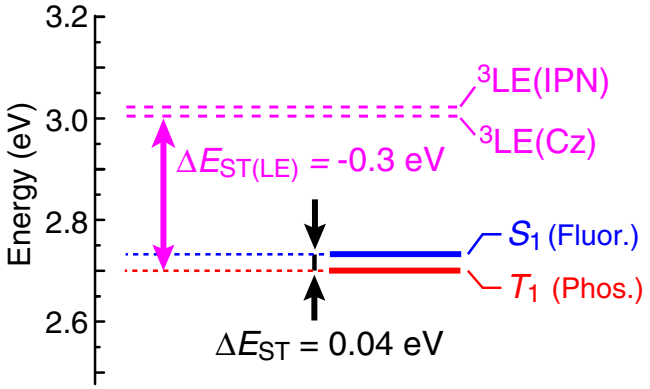

Fig. 4 Energy level diagram of 4CzIPN in toluene. The S_1 and T_1 energies and the ΔE_{ST} value are taken from Ref. 24. The ^{3}LE state at IPN is reported in Ref. 35.

increased in acetonitrile, the other CzBN derivatives showed a decrease of $k_{nr,T}$. Overall, it is clear that $\Phi_{PL,degassed}$ of the three 3CzBN isomers and 4CzBN increased in acetonitrile.

The change in the rate constants in acetonitrile is qualitatively similar to 4CzIPN,[34] implying that solvent effects are a general phenomenon for TADF molecules. The only difference is that the TADF efficiency in toluene, the most nonpolar solvent used by Ishimatsu et al.,[34] demonstrates the best value, suggesting that the absolute value of $\Delta E_{ST(LE)}$ is a minimum in toluene for 4CzIPN, as for 5CzBN. In fact, the ^{3}LE state of 4CzIPN is already above the ^{1}CT and ^{3}CT states (Fig. 4). This result further supports the solvent effect for TADF efficiency and suggests that the most appropriate "solvent environment", that will couple the relevant electronic states, ^{1}CT, ^{3}CT, and ^{3}LE, for TADF efficiency depends on a combination of both the emitter molecules and the solvent.

4 Conclusion

This study examined the solvent dependence of the photophysical properties of a series of CzBN derivatives. Compared with toluene (weakly polar), acetonitrile (strongly polar), which lowers the $\Delta E_{ST(LE)}$, facilitates TADF for *o*-3CzBN and *m*-3CzBN and improves the TADF efficiency for *p*-3CzBN and 4CzBN. Kinetically, these results can be explained by both an increase in k_{RISC} and a decrease in $k_{nr,T}$. However, a strongly polar solvent is not always beneficial for TADF efficiency, as 5CzBN (and also 4CzIPN in Ref. 34) showed a larger decrease in TADF efficiency due to the consequent increase in $k_{nr,T}$. As a result, the polar host environment has an advantage for k_{RISC}, but the appropriate polarity is required for respective molecules to maximize the effect in TADF efficiency. Overall, since close proximity of the ^{3}LE and ^{1}CT states facilitates TADF, its efficiency can be improved by tuning both the ΔE_{ST} and $\Delta E_{ST(LE)}$, which are realized by a combination of (1) the design of the donor-accepter geometry (for ^{1}CT and ^{3}CT) and (2) the selection of donor and accepter moieties (for ^{3}LE).

Acknowledgments

This work was supported, in part, by the International Institute for Carbon Neutral Energy Research (WPI-I2CNER) sponsored by the Ministry of Education, Culture, Sports, Science and Technology (MEXT), and JSPS-KAKENHI Grant Nos. JP16K14102, JP16K17975, and JP17H03137. We would like to thank Editage (www.editage.jp) for English language editing.

References

1. G. N. Lewis, D. Lipkin, and T. T. Magel, "Reversible photochemical processes in rigid media. A study of the phosphorescent state," *J. Am. Chem. Soc.* **63**(11), 3005–3018 (1941).

2. C. A. Parker and C. G. Hatchard, "Triplet-singlet emission in fluid solutions—phosphorescence of eosin," *Trans. Faraday Soc.* **57**(11), 1894–1904 (1961).
3. H. Uoyama et al., "Highly efficient organic light-emitting diodes from delayed fluorescence," *Nature* **492**(7428), 234–238 (2012).
4. C. Adachi, "Third-generation organic electroluminescence materials," *Jpn. J. Appl. Phys.* **53**(6), 060101 (2014).
5. D. Volz, "Review of organic light-emitting diodes with thermally activated delayed fluorescence emitters for energy-efficient sustainable light sources and displays," *J. Photonics Energy* **6**, 020901 (2016).
6. R. Komatsu et al., "Light-blue thermally activated delayed fluorescent emitters realizing a high external quantum efficiency of 25% and unprecedented low drive voltages in OLEDs," *J. Mater. Chem. C* **4**(12), 2274–2278 (2016).
7. Y. J. Xie and Z. Li, "Thermally activated delayed fluorescent polymers," *J. Polym. Sci. Polym. Chem.* **55**(4), 575–584 (2017).
8. Z. Yang et al., "Recent advances in organic thermally activated delayed fluorescence materials," *Chem. Soc. Rev.* **46**(3), 915–1016 (2017).
9. M. Y. Wong and E. Zysman-Colman, "Purely organic thermally activated delayed fluorescence materials for organic light-emitting diodes," *Adv. Mater.* **29**, 1605444 (2017).
10. T. Miwa et al., "Blue organic light-emitting diodes realizing external quantum efficiency over 25% using thermally activated delayed fluorescence emitters," *Sci. Rep.* **7**(1), 284 (2017).
11. H. Nakanotani et al., "Promising operational stability of high-efficiency organic light-emitting diodes based on thermally activated delayed fluorescence," *Sci. Rep.* **3**, 2127 (2013).
12. H. Kaji et al., "Purely organic electroluminescent material realizing 100% conversion from electricity to light," *Nat. Commun.* **6**, 8476 (2015).
13. T. Furukawa et al., "Dual enhancement of electroluminescence efficiency and operational stability by rapid upconversion of triplet excitons in OLEDs," *Sci. Rep.* **5**, 8429 (2015).
14. D. P.-K. Tsang, T. Matsushima, and C. Adachi, "Operational stability enhancement in organic light-emitting diodes with ultrathin Liq interlayers," *Sci. Rep.* **6**, 22463 (2016).
15. F. B. Dias et al., "Triplet harvesting with 100% efficiency by way of thermally activated delayed fluorescence in charge transfer OLED emitters," *Adv. Mater.* **25**(27), 3707–3714 (2013).
16. X. K. Chen et al., "Nature of highly efficient thermally activated delayed fluorescence in organic light-emitting diode emitters: nonadiabatic effect between excited states," *J. Phys. Chem. C* **119**(18), 9728–9733 (2015).
17. T. Ogiwara, Y. Wakikawa, and T. Ikoma, "Mechanism of intersystem crossing of thermally activated delayed fluorescence molecules," *J. Phys. Chem. A* **119**(14), 3415–3418 (2015).
18. J. Gibson, A. P. Monkman, and T. J. Penfold, "The importance of vibronic coupling for efficient reverse intersystem crossing in thermally activated delayed fluorescence molecules," *Chem. Phys. Chem.* **17**(19), 2956–2961 (2016).
19. C. M. Marian, "Mechanism of the triplet-to-singlet upconversion in the assistant dopant ACRXTN," *J. Phys. Chem. C* **120**(7), 3715–3721 (2016).
20. F. B. Dias et al., "The role of local triplet excited states and D-A relative orientation in thermally activated delayed fluorescence: photophysics and devices," *Adv. Sci.* **3**, 1600080 (2016).
21. P. K. Samanta et al., "Up-conversion intersystem crossing rates in organic emitters for thermally activated delayed fluorescence: impact of the nature of singlet vs triplet excited states," *J. Am. Chem. Soc.* **139**(11), 4042–4051 (2017).
22. T. Kobayashi et al., "Contributions of a higher triplet excited state to the emission properties of a thermally activated delayed-fluorescence emitter," *Phys. Rev. Appl.* **7**(3), 034002 (2017).
23. M. K. Etherington et al., "Regio- and conformational isomerization critical to design of efficient thermally-activated delayed fluorescence emitters," *Nat. Commun.* **8**, 14987 (2017).
24. T. Hosokai et al., "Evidence and mechanism of efficient thermally activated delayed fluorescence promoted by delocalized excited states," *Sci. Adv.* **3**(5), e1603282 (2017).

25. Q. Peng et al., "Theoretical study of conversion and decay processes of excited triplet and singlet states in a thermally activated delayed fluorescence molecule," *J. Phys. Chem. C* **121**(25), 13448–13456 (2017).
26. T. Sato et al., "Fluorescence via reverse intersystem crossing from higher triplet states in a bisanthracene derivative," *Sci. Rep.* **7**(1), 4820 (2017).
27. K. Masui, H. Nakanotani, and C. Adachi, "Analysis of exciton annihilation in high-efficiency sky-blue organic light-emitting diodes with thermally activated delayed fluorescence," *Org. Electron.* **14**(11), 2721–2726 (2013).
28. M. Inoue et al., "Effect of reverse intersystem crossing rate to suppress efficiency roll-off in organic light-emitting diodes with thermally activated delayed fluorescence emitters," *Chem. Phys. Lett.* **644**, 62–67 (2016).
29. A. S. D. Sandanayaka et al., "Toward continuous-wave operation of organic semiconductor lasers," *Sci. Adv.* **3**(4), e1602570 (2017).
30. J. R. Lakowicz, *Principles of Fluorescence Spectroscopy*, Chapter 6, 3rd ed., Springer, New York (2006).
31. R. Katoh et al., "Ultrafast relaxation as a possible limiting factor of electron injection efficiency in black dye sensitized nanocrystalline TiO_2 films," *J. Phys. Chem. C* **116**(42), 22301–22306 (2012).
32. T. Yoshihara, S. I. Druzhinin, and K. A. Zachariasse, "Fast intramolecular charge transfer with a planar rigidized electron donor/acceptor molecule," *J. Am. Chem. Soc.* **126**(27), 8535–8539 (2004).
33. Q. Zhang et al., "Design of efficient thermally activated delayed fluorescence materials for pure blue organic light emitting diodes," *J. Am. Chem. Soc.* **134**(36), 14706–14709 (2012).
34. R. Ishimatsu et al., "Solvent effect on thermally activated delayed fluorescence by 1,2,3,5-tetrakis(carbazol-9-yl)-4, 6-dicyanobenzene," *J. Phys. Chem. A* **117**(27), 5607–5612 (2013).
35. H. Hayashi and S. Nagakura, "The E.S.R. and phosphorescence spectra of some dicyanobenzene complexes with methyl-substituted benzenes," *Mol. Phys.* **19**(1), 45–53 (1970).

Takuya Hosokai is a scientist at the National Institute of Advanced Industrial Science and Technology, in Japan. He received his BS and MS degrees in engineering from Niigata University and Yokohama National University in 2003 and 2005, respectively, and his PhD in engineering from Chiba University in 2008. He was a postdoc at Universität Tübingen from 2008 to 2010, where he received a research scholarship from the Alexander von Humboldt Foundation. He is the author of more than 50 journal publications and has written three book chapters. His current research interests include optical and electronic properties of organic semiconducting molecules, and the development of new experimental instruments.

Biographies for the other authors are not available.